Analysis of Downlink Uplink Decoupled Dense Heterogeneous Cellular Network based on User Association using Multi-Slope Path Loss Model

Sundus ALI, Muhammad Imran ASLAM, Irfan AHMED
Department of Electronic Engineering, NED University of Engineering and Technology, Karachi, Pakistan
sundus@neduet.edu.pk

***Abstract*—Keeping in consideration the expected need of node densification of heterogeneous cellular networks in near future, it is imperative that more accurate path loss models be used when analyzing heterogeneous cellular networks performance in terms of user equipment association probability, coverage probability and spectral efficiency. In this paper, we have derived the generalized user equipment association probabilities' expressions of a two-tier Dense Heterogeneous Cellular Network incorporating Downlink Uplink Decoupled technique using multi-slope path loss model, which incorporates the effect of physical environment on the path loss based on separation between transmitter and receiver. For analyzing network performance, we have considered dual-slope and tri-slope path loss models as special cases. The derived analytical expressions have been validated through network simulations and found in good agreement. The results have also been compared with conventional single-slope path loss model and it has been found that the decoupled uplink downlink association probability is higher when incorporating multi-slope path loss model as compared to single-slope path loss model.**

***Index Terms*—cellular networks, probability distribution, propagation losses, stochastic processes, uplink.**

I. INTRODUCTION

In order to offer a promising way of meeting the growing demand of high volume of mobile traffic, data rates and devices and its applications, a complete paradigm shift was imminent. By 2023, it has been forecasted that the mobile data traffic volume will reach 107 exa-bytes per month growing at a compound annual growth rate of 39 percent since 2017 [1]. The average mobile network connection speed is also projected to reach 28.5 megabits per second (Mbps) by 2022, compared to 8.7 Mbps in 2017 [2]. Due to the introduction and popularity of new and bandwidth hungry applications like video streaming, online gaming, interactive web, the demand for higher and robust data rates for end-users is increasing. In recent studies, augmented reality, virtual reality, massive and critical mobile-to-mobile, Internet of Things have been considered as compelling use cases for 5G [3]. As these applications require a fast and reliable uplink connection, with very short time-to-content, it raises question on whether the conventional coupled user association method is applicable or not when catering to time-critical and data hungry applications [4]. To overcome this problem, techniques involving user-centric operation were proposed [5] exploiting decoupling of uplink and downlink connectivity for User Equipment (UE), termed as Downlink Uplink Decoupled (DUDe). In this technique, the UE may associate itself with two Base Stations (BSs) belonging to different tiers for uplink and downlink connectivity based on independent cell association decisions leading to improved uplink network performance [6-8].

Authors in [9-11] have highlighted the benefits of incorporating Downlink Uplink Decoupled (DUDe) technique in multi-tier heterogeneous networks. Some of the advantages include reduced uplink path loss, better Signal to Noise Ratio (SNR), reduced uplink interference level leading to better Signal to Interference Ratio (SIR), better uplink average spectral efficiency and rate, and better utilization of UE power leading to longer battery life. Although it is worth noting that the path loss model used in all the above mentioned work on DUDe as well as in [12-17] is the conventional distance dependent path loss,

$$L = \left(d/d_0\right)^{\alpha} \tag{1}$$

where d_0 is the reference distance (often taken as 1 meter), d is the Euclidean distance between UE and BS and α is the Path Loss Exponent (PLE).

Significant research has been carried out in order to propose more realistic and accurate path loss models over the years [18-20]. Authors in [21, 22] have, through the use of two-ray model, proposed dual-slope path loss model, in which the exponent in the path loss expression is dependent on Transmitter (TX)- Receiver (RX) separation. The experimental work presented in [23, 24] also indicates that the slope for distance dependent path loss does not remain the same against distance.

For ultra-dense networks, authors in [25-29] have analyzed the downlink network performance of single-tier downlink dense cellular networks using multi-slope path loss model. This model takes into consideration, the effect of physical environment like Line-of-Sight (LOS) and non-LOS, buildings, etc. and is hence considered a more realistic and accurate version when compared to single-slope conventional path loss model. Multi-slope path loss model is defined by the PLE whose value is determined with respect to TX-RX distance. In [30, 31], the authors have performed downlink analysis on multi-tier cellular network using multi-slope path loss model.

To the best of our knowledge, the performance of multi-tier DUDe based heterogeneous networks has never been analysed using a path loss model other than the conventional

Digital Object Identifier 10.4316/AECE.2019.02006

distance dependent path loss model. Due to densification of low powered BSs (Small BSs), it is important to analyze the performance of such networks using path loss models which take into account the effects of physical environment. Multi-slope path loss model is a more realistic approach to calculating the increased variations in the link in dense cellular networks. Our contribution is that we have analysed the DUDe based heterogeneous cellular network performance in terms of UE coupled and decoupled association probability, using this more realistic model and also compared the results with that of conventional distance dependent path loss model.

The rest of the paper is organized as follows. Section II describes the system model used to study the performance of DUDe based multi-tier network using multi-slope path loss model. In section III we have derived the general expressions for the UE association probability cases, using multi-slope path loss model as it is a key parameter in assessing the uplink network performance in particular. In section IV, we have further derived the above expressions by taking into account two special cases of multi-slope path loss models namely dual-slope and tri-slope models. In section V, we have presented the simulation results and compared the performance of DUDe based network with conventional distance dependent path loss with that of multi-slope path loss model. Section VI concludes the paper.

II. System Model

In order to analyse the performance of DUDe in multi-tier networks using multi-slope path loss model, we have considered a two-tier network model consisting of Macro Base Stations (MBSs) in one tier and small, low-powered, densely deployed Small Base Stations (SBSs) in the other. For modeling the locations of the BSs, we have used homogeneous Poisson Point Process (PPP), denoted by ϕ_k (where $k = M$ for MBS tier, $k = S$ for SBS tier), having average node densities denoted by λ_k. Fig. 1 shows an instance of PPP generated locations of MBS and SBSs. The analysis is performed on a typical test User Equipment (UE) placed at origin as shown in Fig. 1. The location of a node in the region R^2 is from a realization of ϕ_k, denoted by $x_k = \{x_{k_1}, x_{k_2}\}$.

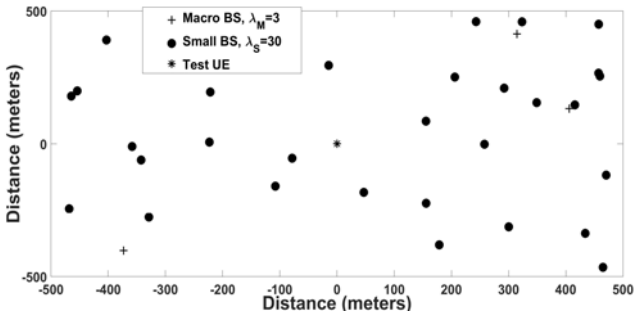

Figure 1. An instance of Poison Point Process based generation of MBSs, and SBSs over an area of 1000×1000 meters with $\tilde{\lambda} = 10$, $\lambda_M = 3$.

The BSs transmit power at P_k and the UEs transmits maximum power at P_d. Fractional power control allows effective use of uplink signal power and prolongs battery life but for the sake of tractability, we have assumed that the UE transmits at maximum power. Universal frequency reuse is assumed where all the BSs transmit using the same operating frequency. Instead of using conventional distance dependent path loss model, $L_{x_k} = \|x_k\|^{-\alpha_k}$ having single slope denoted by $\alpha_k > 2$, we have assumed that the signals in uplink and downlink suffer from multi-slope distance-dependent path loss denoted by:

$$L_n = \prod_{i=1}^{n} R_i^{\alpha_i - \alpha_{i-1}} \|x\|^{-\alpha_n}, 0 \le n \le N-1 \quad (2)$$

where, L_n represents N-slope path loss when $\|x\| \in [R_n, R_{n+1})$, $\prod_{i=1}^{n} R_i^{\alpha_i - \alpha_{i-1}} = 1$ for $n = 0$, $R_0 < R_1 < R_2 ... < R_N = \infty$ and $\alpha_0 \le \alpha_1 \le \alpha_2 ... \le \alpha_{N-1}$

The average downlink and uplink received powers of the signals are respectively given by

$$P_{r_k}^{DL} = P_k h_{x_k} \prod_{i=1}^{n_k} R_i^{\alpha_i - \alpha_{i-1}} \|x_k\|^{-\alpha_{n_k}} \quad (3)$$

$$P_{r_k}^{UL} = P_d h_{x_k} \prod_{i=1}^{n_k} R_i^{\alpha_i - \alpha_{i-1}} \|x_k\|^{-\alpha_{n_k}} \quad (4)$$

where, h_{x_k} represents Rayleigh fading and is an exponentially distributed random variable with a mean of 1. $\|x_k\|$ is Euclidean distance of test UE from the BS located at x_k. The distance distribution of the PPP ϕ_k for nearest serving BS is given by

$$f_{X_k}(x_k) = 2\pi\lambda_k x_k e^{-\pi\lambda_k x_k^2}, x_k \ge 0 \quad (5)$$

$$F_{X_k}(x_k) = 1 - e^{-\pi\lambda_k x_k^2}, x_k \ge 0 \quad (6)$$

When applying DUDe, the user associates with a BS of a certain tier based on the following criteria:

1. The UE will connect to the BS which provides minimum path loss for uplink association.
2. The UE will connect to the BS which is providing maximum average received power for downlink association.

Using the system model, UE association criterion (as shown in Fig. 2), and distance distributions discussed above, we derive the user association probabilities in Section III.

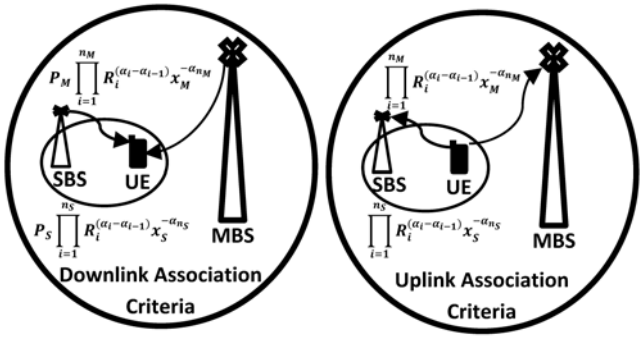

Figure 2. System diagram showing UE association criterion defined for uplink and downlink connectivity for decoupled association

III. User Association Probabilities Using Multi-slope Path Loss Model

In this section, we derive the expressions for probabilities for following four different cases of user associations.

1. Case 1: UE connects to Macro BS in both Uplink and Downlink (coupled association)

2. Case 2:UE connects to Macro BS in Downlink and Small BS in Uplink (decoupled association)
3. Case 3:UE connects to Macro BS Uplink and Small BS in Downlink (decoupled association)
4. Case 4: UE connects to Small BS in both Uplink and Downlink (coupled association)

Case 1:

Probability that the UE will associate itself with the Macro BS in Uplink and Downlink is defined by:

$$P_1 = \Pr(P_M L_M \geq P_S L_S ; L_M \geq L_S) \tag{7}$$

$$P_1 = \Pr(L_M > \frac{P_S}{P_M} L_S ; L_M > L_S) \tag{8}$$

As, $P_S / P_M < 1$, considering the overlap region, we can write (8) as:

$$P_1 = \Pr(L_M > L_S) \tag{9}$$

Putting the value of path losses in (9) from (2), we get the following:

$$P_1 = \Pr\left(\prod_{i=1}^{n_M} R_i^{\alpha_i - \alpha_{i-1}} \left\| x_M \right\|^{-\alpha_{n_M}} > \prod_{j=1}^{n_S} R_j^{\alpha_j - \alpha_{j-1}} \left\| x_S \right\|^{-\alpha_{n_S}} \right) \tag{10}$$

By rearranging the variables, we get:

$$P_1 = \Pr\left(\left\| x_M \right\|^{\alpha_{n_M}} < \frac{\prod_{j=1}^{n_S} R_j^{\alpha_j - \alpha_{j-1}}}{\prod_{i=1}^{n_M} R_i^{\alpha_i - \alpha_{i-1}}} \left\| x_S \right\|^{\alpha_{n_S}} \right) \tag{11}$$

Equation (11) can be further simplified to:

$$P_1 = \Pr\left(x_M < \left(\frac{\prod_{j=1}^{n_S} R_j^{\alpha_j - \alpha_{j-1}}}{\prod_{i=1}^{n_M} R_i^{\alpha_i - \alpha_{i-1}}} \right)^{\frac{1}{\alpha_{n_M}}} x_S^{\frac{\alpha_{n_S}}{\alpha_{n_M}}} \right) \tag{12}$$

Let

$$\tilde{\alpha} = \alpha_{n_S} / \alpha_{n_M} \tag{13}$$

So, (12) becomes,

$$P_1 = \Pr\left(x_M < T^{\frac{c}{\alpha_{n_M}}} x_S^{\tilde{\alpha}} \right) \tag{14}$$

where, c is a constant which takes values +1, –1, and 0 for $n_M > n_S$, $n_M < n_S$, and $n_M = n_S$ respectively, and

$$T = \prod_{i=1}^{|n_S - n_M|} R_{|n_S - n_M|+i-1}^{(\alpha_{|n_S - n_M|+i} - \alpha_{|n_S - n_M|+i-1})} \tag{15}$$

Now, incorporating the distance distribution from (5) into (14), we obtain:

$$P_1 = \int_0^\infty F_{X_M}\left(T^{\frac{c}{\alpha_{n_M}}} x_S \right) f_{x_S^{\tilde{\alpha}}}(x_S^{\tilde{\alpha}}) dx_S^{\tilde{\alpha}} \tag{16}$$

Substituting $v_S = x_S^{\tilde{\alpha}}$ in (16) gives

$$P_1 = \int_0^\infty 2\pi\lambda_S v_S e^{-\pi\lambda_S v_S^2} \left(1 - e^{-\pi\lambda_M T^{\frac{c}{\alpha_{n_M}}} v_S^{2/\tilde{\alpha}}} \right) dv_S \tag{17}$$

$$P_1 = 1 - \int_0^\infty 2\pi\lambda_S v_S e^{-\pi\left(\lambda_M T^{\frac{c}{\alpha_{n_M}}} v_S^{2/\tilde{\alpha}} + \lambda_S v_S^2 \right)} dv_S \tag{18}$$

The integral in (18) cannot be solved in its general form. However, closed form solutions can be obtained for special cases as shown in section IV.

Case 2:

Probability that the UE will associate itself with the Macro BS in Downlink and with Small BS in the Uplink (decoupled association) is defined by:

$$P_2 = \Pr(P_M L_M \geq P_S L_S ; L_M < L_S) \tag{19}$$

After rearranging, we obtain:

$$P_2 = \Pr(L_M \geq \frac{P_S}{P_M} L_S ; L_M < L_S) \tag{20}$$

Considering the overlap region, we can write (20) as:

$$P_2 = \Pr({L_M}^{-1} > {L_S}^{-1}) - \Pr({L_M}^{-1} > \frac{P_M}{P_S} {L_S}^{-1}) \tag{21}$$

Putting the value of path losses in (21) from (2), we get the following:

$$P_2 = \Pr\left(x_M > T^{\frac{c}{\alpha_{n_M}}} x_S^{\tilde{\alpha}} \right) - \Pr\left(x_M > \tilde{P}^{1/\alpha_{n_M}} T^{\frac{c}{\alpha_{n_M}}} x_S^{\tilde{\alpha}} \right) \tag{22}$$

where,

$$\tilde{P} = P_M / P_S \tag{23}$$

Now, incorporating the distance distribution from (5) into (22), we obtain:

$$\begin{aligned} P_2 = & \int_0^\infty \left(1 - F_{X_M}(T^{\frac{c}{\alpha_{n_M}}} x_S) \right) f_{x_S^{\tilde{\alpha}}}(x_S^{\tilde{\alpha}}) dx_S^{\tilde{\alpha}} \\ & - \int_0^\infty \left(1 - F_{X_M}(\tilde{P}^{1/\alpha_{n_M}} T^{\frac{c}{\alpha_{n_M}}} x_S) \right) f_{x_S^{\tilde{\alpha}}}(x_S^{\tilde{\alpha}}) dx_S^{\tilde{\alpha}} \end{aligned} \tag{24}$$

Let $v_S = x_S^{\tilde{\alpha}}$, substituting the values in (24) results in:

$$\begin{aligned} P_2 = & \int_0^\infty 2\pi\lambda_S v_S e^{-\pi\lambda_S v_S^2} (e^{-\pi\lambda_M T^{\frac{c}{\alpha_{n_M}}} v_S^{2/\tilde{\alpha}}}) dv_S - \\ & \int_0^\infty 2\pi\lambda_S v_S e^{-\pi\lambda_S v_S^2} (e^{-\pi\lambda_M \left(\tilde{P}^{2/\alpha_{n_M}} T^{\frac{c}{\alpha_{n_M}}} \right) v_S^{2/\tilde{\alpha}}}) dv_S \end{aligned} \tag{25}$$

Equation (25) can be further simplified to:

$$\begin{aligned} P_2 = & \int_0^\infty 2\pi\lambda_S v_S \, e^{-\pi(\lambda_M T^{\frac{c}{\alpha_{n_M}}} v_S^{2/\tilde{\alpha}} + \lambda_S v_S^2)} dv_S - \\ & \int_0^\infty 2\pi\lambda_S v_S \, e^{-\pi(\lambda_M \tilde{P}^{2/\alpha_{n_M}} T^{\frac{c}{\alpha_{n_M}}} v_S^{2/\tilde{\alpha}} + \lambda_S v_S^2)} dv_S \end{aligned} \tag{26}$$

The integral in (26) cannot be solved in its general form. However, closed form solutions can be obtained for special cases as shown in section IV.

Case 3:

Probability that the UE will associate itself with the Macro BS in Uplink and with Small BS in the Downlink (decoupled association) is defined by:

$$P_3 = \Pr(P_M L_M < P_S L_S ; L_M \geq L_S) \tag{27}$$

After rearranging (27), we get

$$P_3 = \Pr(L_M < \frac{P_S}{P_M} L_S ; L_M \geq L_S) \tag{28}$$

Since there is no overlap region possible for the two conditions shown in (28), the association probability for the case 3 results in zero, i.e.

$$P_3 = 0 \tag{29}$$

Case 4:

Probability that the UE will associate itself with the Small BS in both Uplink and Downlink is defined by:

$$P_4 = \Pr(P_M L_M < P_S L_S ; L_M < L_S) \tag{30}$$

Equation (30) can also be written as:

$$P_4 = \Pr({L_M}^{-1} > \tilde{P} {L_S}^{-1} ; {L_M}^{-1} > {L_S}^{-1}) \tag{31}$$

As, $\tilde{P} > 1$, considering the overlap region, we can write (31) as:

$$P_4 = \Pr({L_M}^{-1} > \tilde{P} {L_S}^{-1}) \tag{32}$$

Putting the value of path losses in (32) from (2), we get the following:

$$P_4 = \Pr\left(x_M > \tilde{P}^{1/\alpha_{n_M}} \overline{T^{\frac{c}{\alpha_{n_M}}}} {x_S}^{\tilde{\alpha}} \right) \tag{33}$$

Now, incorporating the distance distribution from (5) into (33), we obtain:

$$P_4 = \int_0^{\infty} \left(1 - F_{X_M} \left(\tilde{P}^{1/\alpha_{n_M}} \overline{T^{\frac{c}{\alpha_{n_M}}}} x_S \right) \right) f_{{x_S}^{\tilde{\alpha}}}({x_S}^{\tilde{\alpha}}) d{x_S}^{\tilde{\alpha}} \tag{34}$$

Let $v_S = x_S^{\tilde{\alpha}}$, substituting the values in (34), we can derive the case 4 association probability.

$$P_4 = \int_0^{\infty} 2\pi\lambda_S v_S e^{-\pi\left(\lambda_M \tilde{P}^{2/\alpha_{n_M}} \overline{T^{\frac{c}{\alpha_{n_M}}}} v_S^{2/\tilde{\alpha}} + \lambda_S {v_S}^2 \right)} dv_S \tag{35}$$

The integral in (35) cannot be solved in its general form. However, closed form solutions can be obtained for special cases as shown in section IV.

IV. Special Cases: Dual-Slope and Tri-slope Path Loss Models

For the purpose of validating the work shown in section III, we have considered two special cases of multi-slope path loss model namely dual slope path loss model and tri-slope path loss model. The integrals derived in section III for the UE association probabilities are further evaluated in subsequent subsections for these special cases to give an analytical expression for the UE association probabilities in terms of the model parameters.

1. Dual Slope path loss model:

We consider a simple two-ray model with $\alpha_0 = 2$ as used in [26] which exhibit dual slope path loss behavior. In this case,

$$L_k = \begin{cases} \|x_k\|^{-2} & \|x_k\| \leq R_1 \\ {R_1}^{\alpha_1 - 2} \|x_k\|^{-\alpha_1} & \|x_k\| > R_1 \end{cases} \tag{36}$$

where, R_1 represents the critical distance while α_1 represents the PLE when the distance of UE from its serving BS (uplink or downlink) is greater than R_1.

By incorporating the path loss model of (36) in the work done in Section III, we derive first, second and fourth cases of UE association probabilities. We will not evaluate UE association probability for the case 3 in this section as it is zero for the general case as shown in (29).

Case 1:

Referring to (18) for case 1 in section III and considering dual-slope path loss model defined in (36), (9) can be expanded to the following form

$$\begin{aligned} P_1 = {} & \Pr(x_M < x_S ; x_S, x_M \leq R_1) + \Pr(x_M < x_S ; \\ & x_S, x_M > R_1) + \Pr(x_M < {x_S}^{\alpha_1/2} {R_1}^{-\frac{1}{2}(\alpha_1 - 2)} ; \\ & x_M \leq R_1 < x_S) + \Pr(x_M < {x_S}^{2/\alpha_1} {R_1}^{\frac{1}{\alpha_1}(\alpha_1 - 2)} \\ & ; x_S \leq R_1 < x_M) \end{aligned} \tag{37}$$

The last two terms in (37) will become zero considering there is no overlapping region in the events defined for each of them. From the limits set in (37), the integral for the association probability corresponding to case 1 under dual-slope model will take the following form.

$$\begin{aligned} P_1 = {} & \int_0^{R_1} \int_0^{x_S} f_{x_M}(x_M) f_{x_S}(x_S) dx_M dx_S + \\ & \int_{R_1}^{\infty} \int_{R_1}^{x_S} f_{x_M}(x_M) f_{x_S}(x_S) dx_M dx_S \end{aligned} \tag{38}$$

Solving the integral for P_1 in (38), we get:

$$P_1 = \frac{\lambda_M}{\lambda_M + \lambda_S} + e^{-\pi(\lambda_M + \lambda_S) R_1^2} - e^{-\pi\lambda_S R_1^2} \tag{39}$$

Case 2:

Referring to (26) for case 2 in section III and considering dual-slope path loss model defined in (36), (21) can be expanded to the following

$$\begin{aligned} P_2 = {} & \Pr(x_M > x_S ; x_M, x_S \leq R_1) \\ & - \Pr(x_M > \tilde{P}^{1/2} x_S ; x_M, x_S \leq R_1) + \Pr(x_M > x_S ; x_M, x_S > R_1) \\ & - \Pr(x_M > \tilde{P}^{1/\alpha_1} x_S ; x_M, x_S > R_1) + \Pr(x_M > {x_S}^{2/\alpha_1} {R_1}^{\frac{1}{\alpha_1}(\alpha_1 - 2)} \\ & ; x_S \leq R_1 < x_M) - \Pr(x_M > \tilde{P}^{1/\alpha_1} {x_S}^{2/\alpha_1} {R_1}^{\frac{1}{\alpha_1}(\alpha_1 - 2)} \\ & ; x_S \leq R_1 < x_M) + \Pr(x_M > {x_S}^{\alpha_1/2} {R_1}^{-\frac{1}{2}(\alpha_1 - 2)} \\ & ; x_M \leq R_1 < x_S) - \Pr(x_M > \tilde{P}^{1/2} {x_S}^{\alpha_1/2} {R_1}^{-\frac{1}{2}(\alpha_1 - 2)} \\ & ; x_M \leq R_1 < x_S) \end{aligned} \tag{40}$$

Some of terms in (40) will become zero considering there is no overlap region in the events defined for them. From the limits set in (40) and considering the overlap regions corresponding to each probability terms, the integral will take the following form

$$P_2 = \int_0^{R_1}\int_{x_S}^{R_1} f_{x_M}(x_M) f_{x_S}(x_S) dx_M\, dx_S - \int_0^{R_1}\int_{\tilde{P}^{1/\alpha_0} x_S}^{R_1} f_{x_M}(x_M) f_{x_S}(x_S) dx_M\, dx_S + \int_{R_1}^{\infty}\int_{x_S}^{\infty} f_{x_M}(x_M) f_{x_S}(x_S) dx_M\, dx_S - \int_{R_1}^{\infty}\int_{\tilde{P}^{1/\alpha_1} x_S}^{\infty} f_{x_M}(x_M) f_{x_S}(x_S) dx_M\, dx_S - \int_{\tilde{P}^{-1/2} R_1}^{R_1}\int_{R_1}^{\tilde{P}^{1/\alpha_1} x_S} f_{x_M}(x_M) f_{x_S}(x_S) dx_M\, dx_S \quad (41)$$

Solving the integral in (41), we get

$$P_2 = \frac{\lambda_S}{\lambda_M+\lambda_S} - \frac{\lambda_S}{\lambda_M \tilde{P}+\lambda_S}(1-e^{-\pi(\lambda_M\tilde{P}+\lambda_S)R_1^2}) + e^{-\pi(\lambda_M+\lambda_S)R_1^2} - e^{-\pi(\lambda_M+\lambda_S\tilde{P}^{-1})R_1^2} - \frac{\lambda_S}{\lambda_M \tilde{P}^{2/\alpha_1}+\lambda_S}\begin{pmatrix} 2e^{-\pi(\lambda_M\tilde{P}^{2/\alpha_1}+\lambda_S)R_1^2} \\ -e^{-\pi(\lambda_M\tilde{P}^{2/\alpha_1}+\lambda_S)\tilde{P}^{-1}R_1^2}\end{pmatrix} \quad (42)$$

Case 4:

Incorporating the dual-slope path loss model given in (36) in the general case expression derived in (35) for UE association probability of case 4, (32) can be expanded to the following:

$$\begin{aligned} P_4 &= \Pr(x_M > \tilde{P}^{1/2}x_S; x_M, x_S \le R_1) \\ &+ \Pr(x_M > \tilde{P}^{1/\alpha_1}x_S; x_M, x_S > R_1) \\ &+ \Pr(x_M > \tilde{P}^{1/\alpha_1}x_S^{2/\alpha_1}R_1^{1/\alpha_1(\alpha_1-2)}; x_S \le R_1 < x_M) \\ &+ \Pr(x_M > \tilde{P}^{1/2}x_S^{\alpha_1/2}R_1^{-1/2(\alpha_1-2)}; x_M \le R_1 < x_S) \end{aligned} \quad (43)$$

Some of terms in (43) will become zero considering there is no overlap region for the events defined for them. From the limits set in (43), the integral will take the following form

$$P_4 = \int_0^{R_1}\int_{\tilde{P}^{1/2}x_S}^{R_1} f_{x_M}(x_M) f_{x_S}(x_S) dx_M\, dx_S + \int_{R_1}^{\infty}\int_{\tilde{P}^{1/\alpha_1}x_S}^{\infty} f_{x_M}(x_M) f_{x_S}(x_S) dx_M\, dx_S + \int_{\tilde{P}^{-1/2}R_1}^{R_1}\int_{R_1}^{\tilde{P}^{1/\alpha_1}R_1} f_{x_M}(x_M) f_{x_S}(x_S) dx_M\, dx_S \quad (44)$$

Solving the integral in (44), we get:

$$P_4 = \frac{\lambda_S}{\lambda_M\tilde{P}+\lambda_S}(1-e^{-\pi(\lambda_M\tilde{P}+\lambda_S)R_1^2}) + \frac{2\lambda_S}{\lambda_M\tilde{P}^{2/\alpha_1}+\lambda_S}(e^{-\pi(\lambda_M\tilde{P}^{2/\alpha_1}+\lambda_S)R_1^2}) - e^{-\pi\lambda_M R_1^2} + 2e^{-\pi(\lambda_M+\lambda_S)R_1^2} - e^{-\pi(\lambda_M+\lambda_S\tilde{P}^{-1})R_1^2}) - \frac{\lambda_S}{\lambda_M\tilde{P}^{2/\alpha_1}+\lambda_S}(e^{-\pi(\lambda_M\tilde{P}^{2/\alpha_1}+\lambda_S)R_1^2\tilde{P}^{-1}}) \quad (45)$$

2. Tri-Slope path loss model:

Here, we combine a simple two-ray model with bounded path loss model as used in [26] to simulate a tri-slope path loss behavior where, $\alpha_0 = 0$. In this case,

$$L_k = \begin{cases} 1 & \|x_k\| \le R_1 \\ R_1^{\alpha_1}\|x_k\|^{-\alpha_1} & R_2 \ge \|x_k\| > R_1 \\ R_1^{\alpha_1}R_2^{\alpha_2-\alpha_1}\|x_k\|^{-\alpha_2} & \|x_k\| > R_2 \end{cases} \quad (46)$$

where, R_1 and R_2 represent the critical distances while α_1 and α_2 represent the corresponding PLEs. Incorporating (46) in the work done in section III, we derive first, second and fourth cases of UE association probabilities. We will not evaluate UE association probability for the case 3 in this section as it is zero for the general case as shown in (29).

Case 1:

For finding case 1 association probability using tri-slope path loss model, we focus on regions where $x_M \le x_S$, referring to (9) we can obtain the following expression for P_1:

$$\begin{aligned} P_1 &= \Pr(x_M < x_S; x_S, x_M \le R_1) + \Pr(x_M < x_S; \\ &R_1 < x_S, x_M \le R_2) + \Pr(x_M < x_S; x_S, x_M > R_2) + \\ &\Pr(x_M < x_S^{\alpha_2/\alpha_1}R_2^{-1/\alpha_1(\alpha_2-\alpha_1)}; R_1 < x_M \le R_2, x_S > R_2) \end{aligned} \quad (47)$$

By solving (47), we get the following:

$$P_1 = \frac{\lambda_M}{\lambda_M+\lambda_S} + e^{-\pi(\lambda_M+\lambda_S)R_1^2} - e^{-\pi\lambda_S R_1^2} + e^{-\pi(\lambda_M+\lambda_S)R_2^2} - e^{-\pi(\lambda_M R_1^2+\lambda_S R_2^2)} \quad (48)$$

Case 2:

For finding case 2 association probability using tri-slope path loss model, we focus on regions where $x_S \le x_M$, we can obtain the following expression for P_2

$$\begin{aligned} P_2 &= \Pr(x_M > x_S; x_M, x_S \le R_1) + \Pr(x_M > x_S; \\ &R_1 < x_M, x_S \le R_2) - \Pr(x_M > \tilde{P}^{1/\alpha_1}x_S; R_1 < x_M, x_S \le R_2) + \\ &\Pr(x_M > x_S; x_M, x_S > R_2) - \Pr(x_M > \tilde{P}^{1/\alpha_2}x_S; x_M, x_S > R_2) \\ &+ \Pr(x_M > R_1; x_S \le R_1, R_1 < x_M \le R_2) - \Pr(x_M > \tilde{P}^{1/\alpha_1}R_1; \\ &x_S \le R_1, R_1 < x_M \le R_2) + \Pr(x_M > R_1^{\alpha_1/\alpha_2}R_2^{1/\alpha_2(\alpha_2-\alpha_1)}; \\ &x_M > R_2, x_S \le R_1) - \Pr(x_M > \tilde{P}^{1/\alpha_2}R_1^{\alpha_1/\alpha_2}R_2^{1/\alpha_2(\alpha_2-\alpha_1)}; \\ &x_M > R_2, x_S \le R_1) + \Pr(x_M > x_S^{\alpha_1/\alpha_2}R_2^{1/\alpha_2(\alpha_2-\alpha_1)}; x_M > R_2 \\ &, R_1 < x_S \le R_2) - \Pr(x_M > \tilde{P}^{1/\alpha_2}x_S^{\alpha_1/\alpha_2}R_2^{1/\alpha_2(\alpha_2-\alpha_1)}; \\ &x_M > R_2, R_1 < x_S \le R_2) \end{aligned} \quad (49)$$

By solving (49), we get the following

$$P_2 = \frac{\lambda_S}{\lambda_M+\lambda_S} - \frac{2\lambda_S}{\lambda_M\tilde{P}^{2/\alpha_1}+\lambda_S}e^{-\pi(\lambda_M\tilde{P}^{2/\alpha_1}+\lambda_S)R_1^2} - \frac{2\lambda_S}{\lambda_M\tilde{P}^{2/\alpha_2}+\lambda_S}e^{-\pi(\lambda_M\tilde{P}^{2/\alpha_2}+\lambda_S)R_2^2} + \frac{\lambda_S}{\lambda_M\tilde{P}^{2/\alpha_1}+\lambda_S} e^{-\pi(\lambda_M\tilde{P}^{2/\alpha_1}+\lambda_S)R_2^2} + \frac{\lambda_S e^{-\pi(\lambda_M\tilde{P}^{2/\alpha_2}+\lambda_S)R_2^2\tilde{P}^{-2/\alpha_1}}}{\lambda_M\tilde{P}^{2/\alpha_2}+\lambda_S} + e^{-\pi(\lambda_M+\lambda_S)R_1^2} + e^{-\pi(\lambda_M+\lambda_S)R_2^2} - e^{-\pi(\lambda_M+\lambda_S\tilde{P}^{-2/\alpha_1})R_2^2} \quad (50)$$

Case 4:

For finding case 4 association probability using tri-slope path loss model, again we focus on regions where $x_M \le x_S$, we can obtain the following expression for P_4:

$$\begin{aligned} P_4 = {} & \Pr(x_M > \tilde{P}^{1/\alpha_1} x_S; R_1 < x_M, x_S \le R_2) + \\ & \Pr(x_M > \tilde{P}^{1/\alpha_2} x_S; x_M, x_S > R_2) + \Pr(x_M > \tilde{P}^{1/\alpha_1} R_1; \\ & x_S \le R_1, R_1 < x_M \le R_2) + \Pr(x_M > \tilde{P}^{1/\alpha_2} R_1^{\alpha_1/\alpha_2} R_2^{1/\alpha_2(\alpha_2-\alpha_1)} \\ & ; x_M > R_2, x_S \le R_1) + \Pr(x_M > \tilde{P}^{1/\alpha_2} x_S^{\alpha_1/\alpha_2} R_2^{1/\alpha_2(\alpha_2-\alpha_1)} \\ & ; x_M > R_2, R_1 < x_S \le R_2) \end{aligned} \quad (51)$$

By solving (51), we get the following:

$$\begin{aligned} P_4 = {} & \frac{\lambda_S}{\lambda_M \tilde{P}^{2/\alpha_1} + \lambda_S} (e^{-\pi(\lambda_M \tilde{P}^{2/\alpha_1} + \lambda_S) R_1^2} \\ & - e^{-\pi(\lambda_M \tilde{P}^{2/\alpha_1} + \lambda_S) R_2^2}) + \frac{\lambda_S}{\lambda_M \tilde{P}^{2/\alpha_2} + \lambda_S} e^{-\pi(\lambda_M \tilde{P}^{2/\alpha_2} + \lambda_S) R_2^2} \\ & + e^{-\pi(\lambda_M \tilde{P}^{2/\alpha_2} + \lambda_S) R_2^2} - e^{-\pi(\lambda_M \tilde{P}^{2/\alpha_1} + \lambda_S) R_1^2} \\ & + 2e^{-\pi(\lambda_M + \lambda_S \tilde{P}^{-2/\alpha_1}) R_2^2} - e^{-\pi(\lambda_M + \lambda_S) R_2^2} \\ & + e^{-\pi\lambda_M \tilde{P}^{2/\alpha_1} R_1^2} - e^{-\pi(\lambda_M \tilde{P}^{2/\alpha_2} + \lambda_S \tilde{P}^{-2/\alpha_1}) R_2^2} - e^{-\pi\lambda_M R_2^2} \end{aligned} \quad (52)$$

V. Simulation Results and Discussion

In order to validate the analytical findings, we have run Monte Carlo simulations with 10000 instances. For every instance, we have considered a two-tier network containing MBSs and SBSs having different SBS densities $\lambda_S = 3, 30, 60, 90, 120, 180$, with $\lambda_M = 3$. The BSs' locations have been determined using Homogeneous Poisson Point Process. The SBS transmit powers have been defined as $P_S = 30dBm, 24\text{dBm}$, and MBS transmit power as $P_M = 46dBm$. We have considered two PLE values for single-slope path loss model, $\alpha = 3$ and $\alpha = 4$. For dual-slope path loss model we have set the critical distance $R_1 = 1m$ and PLEs have been set to $[\alpha_0, \alpha_1] = [2, 4]$ representing bounded path loss model as discussed in [26]. For the tri-slope path loss model, we have considered critical distances at $R_1 = 1m$ and $R_2 = 267m$ and PLE values have been set to $[\alpha_0, \alpha_1, \alpha_2] = [0, 2, 4]$ representing the combination of classic two-ray model and bounded path loss model as discussed in [26].

We have compared the UE association probabilities of first, second and fourth cases using single-slope, dual-slope and tri-slope path loss models. The association probabilities for each of the cases are defined as the percentage of devices (UEs) that will be associated with the particular case.

In Fig. 3, we have compared the UE association probabilities of cases 2 and 4 using single-slope and dual-slope path loss models against different values of BS density ratios $\tilde{\lambda}$ at $\tilde{P} = 40$. It has been found that case 1 association probability remains unchanged for different path loss models hence not plotted in Fig. 3. The values of $\tilde{\lambda}$ have been chosen so as to simulate moderate to ultra-dense network scenarios. We use the UE association probability expressions derived in [4] for single-slope path loss model.

As indicated in Fig. 3, case 2 association probability (decoupled) increases when using dual-slope path loss model. This indicates that the DUDe performance is better when using a more accurate (two-ray) path loss model as compared to single-slope path loss model which uses an approximated PLE value (between 2 and 4). On the other hand the case 2 association probability is highest around $\tilde{\lambda} = 10$ but drops steadily with increase in $\tilde{\lambda}$, resulting in an increase in case 4 association probability (i.e. coupled association).

Fig. 4, shows a comparison of the UE association probabilities of cases 2 and 4 using single slope and tri-slope path loss models against different values of BS density ratios. Again, case 1 association probability (coupled association) remains unchanged with respect to the path loss model used and hence has not been shown in Fig. 4. As shown in Fig. 4, case 2 association probability has been found to be significantly higher when incorporating tri-slope path loss model as compared to single-slope model at both $\alpha = 3$ and $\alpha = 4$. Case 4 association probability is computed to be nearly zero indicating that the UEs will normally associate with SBSs in decoupled mode when tri-slope model is being considered.

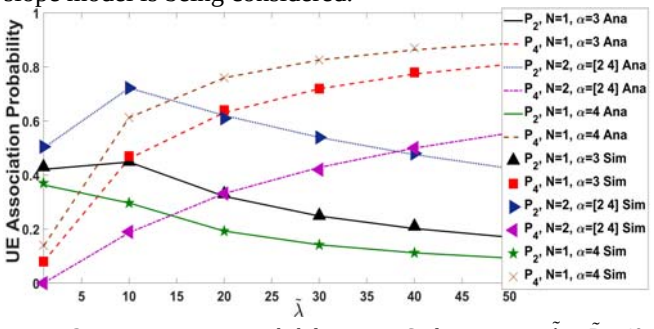

Figure 3. UE association probability vs. BS density ratio $\tilde{\lambda}$ at $\tilde{P} = 40$. Here P_2 and P_4 are case 2 and case 4 association probabilities respectively and N represents the order of slope for the path loss model. Two path loss models have been compared which includes single-slope model with $\alpha = 3$, $\alpha = 4$ and dual-slope model with $[\alpha_0, \alpha_1] = [2, 4]$ and $R_1 = 1m$

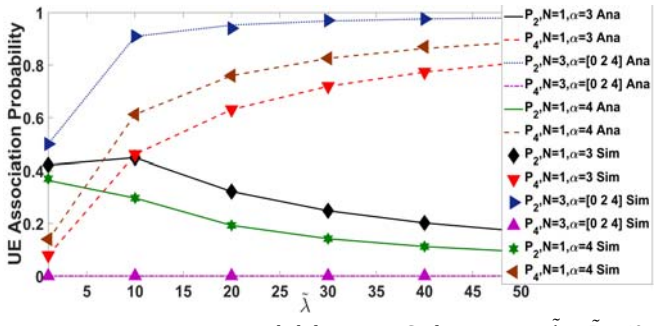

Figure 4. UE association probability vs. BS density ratio $\tilde{\lambda}$ at $\tilde{P} = 40$. Here P_2 and P_4 are case 2 and case 4 association probabilities respectively and N represents the order of slope for the path loss model. Two path loss models have been compared which includes single-slope model with $\alpha = 3$, $\alpha = 4$ and tri-slope model with $[\alpha_0, \alpha_1, \alpha_2] = [0, 2, 4]$ and $R_1 = 1m$ and $R_2 = 267m$.

In Fig. 5 and Fig. 6, we have compared case 2 UE association probabilities (SBS for uplink and MBS for downlink) versus the BS density ratio $\tilde{\lambda}$ for single and dual slope path loss models for different values of $\tilde{P}$. As seen in the figures, higher values of case 2 association probability are obtained when considering dual-slope path loss model as compared to single slope models with $\alpha = 3$ and $\alpha = 4$. The probability also increase with an increase in $\tilde{P}$ which

represents lower SBS transmit power. Moreover, for each value of $\tilde{P}$, the case 2 association probability increases till $\tilde{\lambda}=10$, and then steadily decreases as $\tilde{\lambda}$ increases to higher values indicative of dense cellular network. Hence it may be concluded that low powered node densification will not increase the likelihood of decoupled uplink downlink association for UEs, rather it will result in an increase in case 4 association probability which indicates coupled association with SBS as further elaborated in figures 7 and 8.

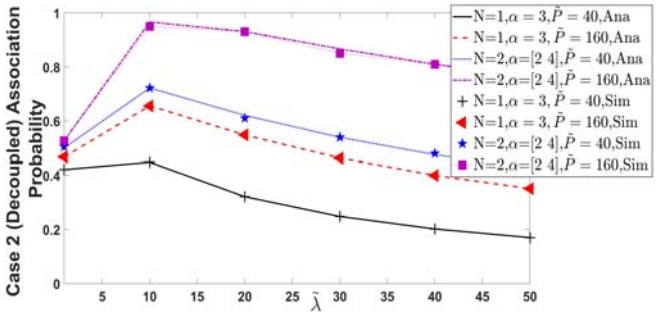

Figure 5. Case 2 UE association probability vs. BS density ratio $\tilde{\lambda}$ for different values of $\tilde{P}$. Here, *N* represents the order of slope for the path loss model. Two path loss models have been compared which includes single-slope model with $\alpha=3$ and dual-slope model with $[\alpha_0,\alpha_1]=[2,4]$ and $R_1=1m$

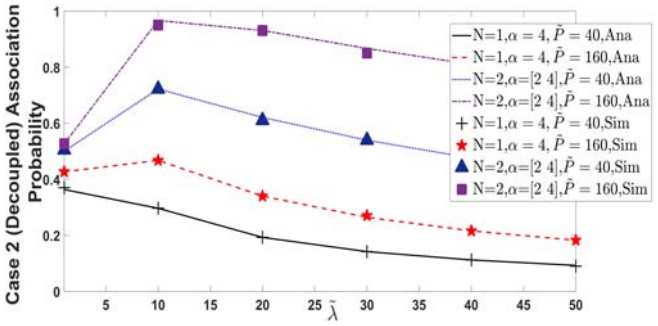

Figure 6. Case 2 UE association probability vs. BS density ratio $\tilde{\lambda}$ for different values of $\tilde{P}$. Here, *N* represents the order of slope for the path loss model. Two path loss models have been compared which includes single-slope model with $\alpha=4$ and dual-slope model with $[\alpha_0,\alpha_1]=[2,4]$ and $R_1=1m$

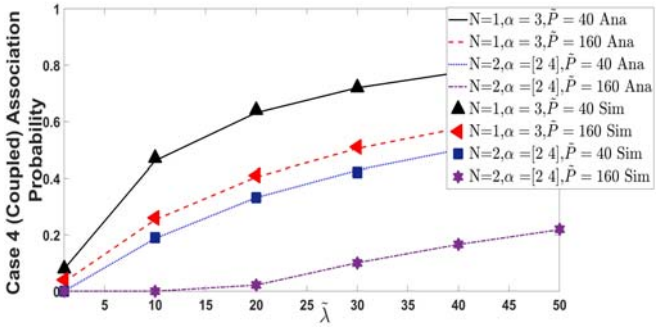

Figure 7. Case 4 UE association probability vs. BS density ratio $\tilde{\lambda}$ for different values of $\tilde{P}$. Here, *N* represents the order of slope for the path loss model. Two path loss models have been compared which includes single-slope model with $\alpha=3$ and dual-slope model with $[\alpha_0,\alpha_1]=[2,4]$ and $R_1=1m$

In Fig. 7 and Fig. 8, we have compared case 4 UE association probability (SBS for both uplink and downlink) versus $\tilde{\lambda}$ for single and dual slope path loss models for different values of $\tilde{P}$. As seen in the figures, lower values of case 4 association probabilities are obtained when considering dual-slope path loss model as compared to single slope models with $\alpha=3$ and $\alpha=4$.

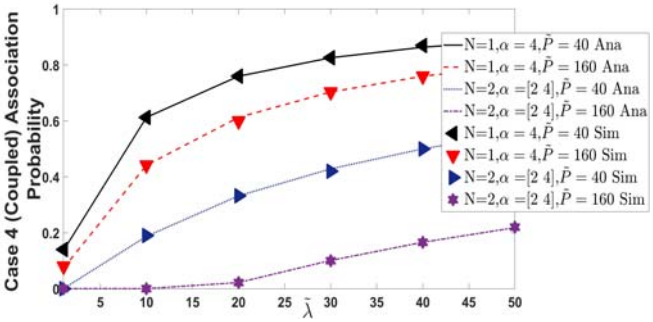

Figure 8. Case 4 UE association probability vs. BS density ratio $\tilde{\lambda}$ for different values of $\tilde{P}$. Here, *N* represents the order of slope for the path loss model. Two path loss models have been compared which includes single-slope model with $\alpha=4$ and dual-slope model with $[\alpha_0,\alpha_1]=[2,4]$ and $R_1=1m$

The probability also decreases with an increase in $\tilde{P}$ but rises with increase in $\tilde{\lambda}$ indicative of more UEs expected to connect to SBS in coupled mode.

VI. Conclusion

In this paper, we have derived the UE association probabilities of a two-tier Heterogeneous Cellular Network incorporating DUDe technique using multi-slope path loss model. In order to analyze the network performance in terms of decoupled association, we have considered two special cases of this model namely, dual-slope and tri-slope path loss. The analytical results obtained in this work are compared with simulated values and are found in good agreement. The simulations as well as the analytical results indicate a drastic difference in the values of decoupled association probabilities (case 2) when using multi-slope path loss model as compared to single-slope path loss model, which is considered an approximation. As a result, the multi-slope path loss model is considered to be more realistic and accurate as it provides better insight into the performance of DUDe based heterogeneous cellular networks. Our work shows that DUDe will perform better in realistic environments, which are better modeled through dual or tri-slope path loss models.

References

[1] F. Jejdling, "Ericsson Mobility Report," Document ID: EAB-18:004510 Uen, June 2018.

[2] Cisco, "Cisco Visual Networking Index: Forecast and Trends,2017–2022," Document ID:1543280537836565, November 26, 2018

[3] J. Orlosky, K. Kiyokawa, H. Takemura, "Virtual and Augmented Reality on the 5G Highway," Journal of Information Processing, vol. 25, pp. 133-141, 2017. doi:10.2197/ipsjjip.25.133

[4] K. Smiljkovikj, P. Popovski, L. Gavrilovska, "Analysis of the Decoupled Access for Downlink and Uplink in Wireless Heterogeneous Networks," IEEE Wireless Communication Letters, vol. 4, no. 2, pp. 173-176, 2015. doi:10.1109/LWC.2015.2388676

[5] S. Singh, X. Zhang, J. G. Andrews, "Joint rate and SINR coverage analysis for decoupled uplink-downlink biased cell associations in HetNets," IEEE Transactions on Wireless Communication, vol. 14, no. 10, pp. 5360-5373, 2015. doi:10.1109/TWC.2015.2437378

[6] M. N. Sial, J. Ahmed, "Analysis of K-tier 5G heterogeneous cellular network with dual-connectivity and uplink–downlink decoupled access," Journal on Telecommunication Systems, vol. 67, no. 4, pp. 669-685, 2018. doi:10.1007/s11235-017-0368-2

[7] M. N. Sial, J. Ahmed, "A Realistic Uplink–Downlink Coupled and Decoupled User Association Technique for K-tier 5G HetNets,"

Arabian Journal for Science and Engineering, vol. 43, no. 6, pp 1–20, 2018.doi:10.1007/s13369-018-3339-3

[8] M. Sial and J. Ahmed, A novel and realistic hybrid downlink-uplink coupled / decoupled access scheme for 5G HetNets. Turkish Journal on Electrical and Computer Engineering, vol. 25, no. 6, pp. 4457 – 4473, 2017. doi:10.3906/elk-1612-167

[9] F. Boccardi, J. Andrews, H. Elshaer, M. Dohler, S. Parkvall, P. Popovski, S. Singh, "Why to decouple the uplink and downlink in cellular networks and how to do it," IEEE Communication Magazine, vol. 54, no. 3, pp. 110-117, 2016. doi:10.1109/MCOM.2016.7432156

[10] J. G. Andrews, S. Buzzi, W. Choi, S. V. Hanly, A. Lozano, A. C. K. Soong, J. C. Zhang, "What Will 5G Be?," IEEE Journal on Selected Areas in Communications, vol. 32, no. 6, pp. 1065-1082, 2014.doi:10.1109/JSAC.2014.2328098

[11] I. Chih-Lin, S. Han, Z. Xu, S. Wang, Q. Sun, Y. Chen, "New paradigm of 5G wireless internet," IEEE Journal on Selected Areas of Communication, vol. 34, no. 3, pp. 474-482, 2016. doi:10.1109/JSAC.2016.2525739

[12] M. Bacha, Y. Wu, B. Clerckx, "Downlink and uplink decoupling in two-tier heterogeneous networks with multi-antenna base stations," IEEE Transactions on Wireless Communication, vol. 16, no. 5, pp. 2760-2775, 2017. doi:10.1109/TWC.2017.2665466

[13] L. Zhang, W. Nie, G. Feng, F.-C. Zheng, S. Qin, "Uplink performance improvement by decoupling uplink/downlink access in HetNets," IEEE Transactions on Vehicular Technology, vol. 66, no. 8, pp. 6862-6876, 2017. doi:10.1109/TVT.2017.2653799

[14] H. Elshaer, M. N. Kulkarni, F. Boccardi, J. G. Andrews, M. Dohler, "Downlink and uplink cell association with traditional macrocells and millimeter wave small cells," IEEE Transactions on Wireless Communication, vol. 15, no. 9, pp. 6244-6258, 2016. doi:10.1109/TWC.2016.2582152

[15] M. Di Renzo, P.Guan, "Stochastic geometry modeling and system-level analysis of uplink heterogeneous cellular networks with multi-antenna base stations," IEEE Transactions on Communication vol. 64, no. 6, pp. 2453-2476, 2016. doi:10.1109/TCOMM.2016.2552163

[16] J. Park, S.-L. Kim, J. Zander, "Tractable resource management with uplink decoupled millimeter-wave overlay in ultra-dense cellular networks," IEEE Transactions on Wireless Communication, vol. 15, no. 6, pp. 4362-4379, 2016. doi:10.1109/TWC.2016.2540626

[17] X. Sui, Z. Zhao, R. Li, H. Zhang, "Energy efficiency analysis of heterogeneous cellular networks with downlink and uplink decoupling," IEEE Global Communications Conference, pp. 1-7, 2015. doi:10.1109/GLOCOM.2015.7417361

[18] H. H. Xia, "A simplified analytical model for predicting path loss in urban and suburban environments," IEEE Transactions on Vehicular Technology, vol. 46, no. 4, pp. 1040-1046, 1997. doi:10.1109/25.653077

[19] V. Erceg, L. J. Greenstein, S. Y. Tjandra, S. R. Parkoff, A. Gupta, B. Kulic, A. A. Julius, R. Bianchi, "An empirically based path loss model for wireless channels in suburban environments," IEEE Journal on Selected Areas in Communications, vol. 17, no. 7, pp. 1205-1211, 1999. doi:10.1109/49.778178

[20] T. K. Sarkar, J. Zhong, K. Kyungjung, A. Medouri, M. Salazar-Palma, "A survey of various propagation models for mobile communication," IEEE Antennas and Propagation Magazine, vol. 45, no. 3, pp. 51-82, 2003. doi:10.1109/MAP.2003.1232163

[21] T. S. Rappaport, L. B. Milstein, "Effects of radio propagation path loss on DS-CDMA cellular frequency reuse efficiency for the reverse channel," IEEE Transactions on Vehicular Technology, vol. 41, no. 3, pp. 231-242, 1992. doi:10.1109/25.155970

[22] H. Xia, H. L. Bertoni, L. R. Maciel, A. Lindsay-Stewart, R. Rowe, "Radio propagation characteristics for line-of-sight microcellular and personal communications," IEEE Transactions on Antennas and Propagation, vol. 41, no. 10, pp. 1439-1447, 1993. doi:10.1109/8.247785

[23] V. Erceg, S. Ghassemzadeh, M. Taylor, D. Li, D. L. Schilling, "Urban/suburban out-of-sight propagation modeling," IEEE Communications Magazine, vol. 30, no. 6, pp. 56-61, 1992. doi:10.1109/35.141584

[24] M. J. Feuerstein, K. L. Blackard, T. S. Rappaport, S. Y. Seidel, H. H. Xia, "Path loss, delay spread, and outage models as functions of antenna height for microcellular system design," IEEE Transactions on Vehicular Technology, vol. 43, no. 3, pp. 487-498, 1994. doi:10.1109/25.312809

[25] A. K. Gupta, X. Zhang, J. G. Andrews, "SINR and Throughput Scaling in Ultradense Urban Cellular Networks," IEEE Wireless Communications Letters, vol. 4, no. 6, pp. 605-608, 2015. doi:10.1109/LWC.2015.2472404

[26] X. Zhang, J. G.Andrews, "Downlink Cellular Network Analysis With Multi-Slope Path Loss Models," IEEE Transactions on Communication, vol. 63, no. 5, pp. 1881-1894, 2015. doi:10.1109/TCOMM.2015.2413412

[27] V. M. Nguyen, M. Kountouris, "Coverage and capacity scaling laws in downlink ultra-dense cellular networks," IEEE International Conference on Communications, pp. 1-7, 2016. doi:10.1109/ICC.2016.7510958

[28] A. A. Ammouri, J. G. Andrews, F. Baccelli, "A Unified Asymptotic Analysis of Area Spectral Efficiency in Ultradense Cellular Networks," IEEE Transactions on Information Theory, pp. 1-1, 2018. doi:10.1109/TIT.2018.2845380

[29] B. Yang, G. Mao, M. Ding, X. Ge, X. Tao, "Dense Small Cell Networks: From Noise-Limited to Dense Interference-Limited," IEEE Transactions on Vehicular Technology, vol. 67, no. 5, pp. 4262-4277, 2018. doi:10.1109/TVT.2018.2794452

[30] H. Munir, S. A. Hassan, H. Pervaiz, Q. Ni, L. Musavian, "Resource optimization in multi-tier HetNets exploiting multi-slope path loss model," IEEE Access vol. 5, pp. 8714-8726, 2017. doi:10.1109/ACCESS.2017.2699941

[31] H. Munir, S. A. Hassan, H. Pervaiz, Q. Ni, L. Musavian, "User association in 5G heterogeneous networks exploiting multi-slope path loss model," Recent Trends in Telecommunications Research, pp. 1-5, 2017. doi:10.1109/RTTR.2017.7887875.